

Reprint 508

Observation of sea breeze interactions  
at and near Hong Kong International Airport

O.S.M. Lee & C.M. Shun

Meteorological Applications Vol. 10, p.p. 1-9, 2003

*Copyright of Royal Meteorological Society*

# Observation of sea breeze interactions at and near Hong Kong International Airport

O Lee and C M Shun

Hong Kong Observatory, 134A Nathan Road, Kowloon, Hong Kong, China  
cmshun@hko.gov.hk

Hong Kong International Airport (HKIA) is located in a coastal environment and is occasionally affected by sea breezes. High air temperatures relative to sea surface temperature, coupled with light winds or moderate east to northeasterly winds are favourable conditions for the development of a sea breeze at the airport. In the afternoon of 27 April 2000, sea breezes affected the airport and a sea breeze front was formed by convergence between the westerly sea breeze and strengthening easterlies. An aircraft landing at HKIA encountered the sea breeze front and reported wind shear with airspeed gain of up to 15 kt at a height of 30 m (100 feet) above ground. Surface wind observations and Doppler velocity data of a Terminal Doppler Weather Radar (TDWR) allow quantitative analysis of the wind shear event. Shortly after the wind shear event, the TDWR also captured interesting interactions between the sea breeze front and an area of passing showers. This paper presents a quantitative analysis of the wind shear event and observations of the sea breeze interactions by the TDWR.

## 1. Geographical location and meteorological observations

Figure 1 shows the location of HKIA at Chek Lap Kok (CLK). The airport is situated on an island which was

partly reclaimed from the sea, to the immediate north of Lantau Island. A larger land mass connected to the mainland lies to the northeast of the airport. The airport has two parallel runways – Northern Runway 07L/25R and Southern Runway 07R/25L (Figure 1).

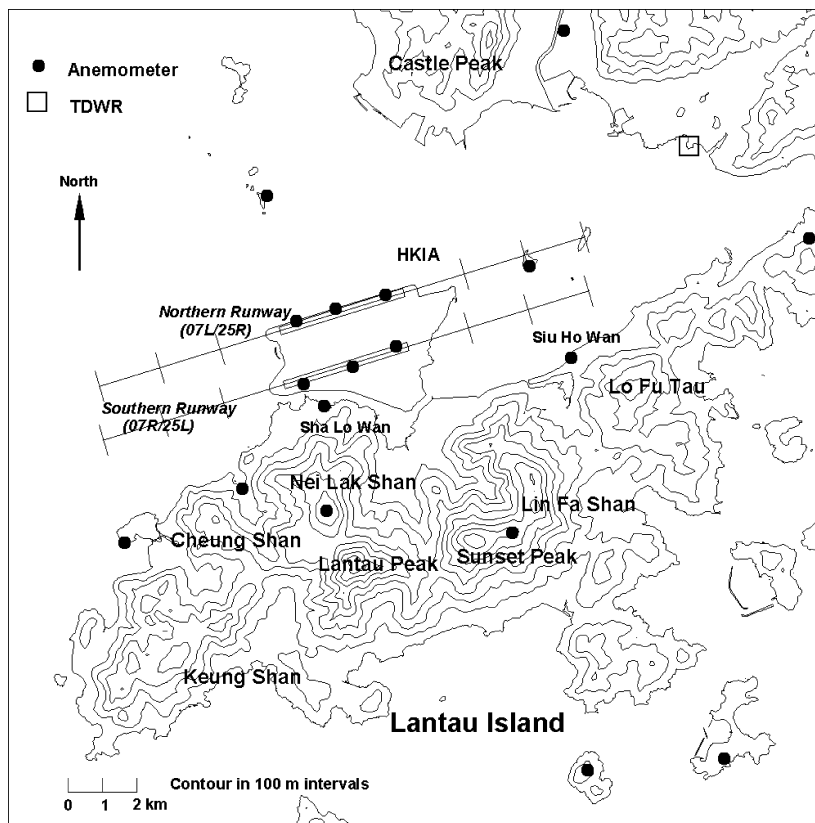


Figure 1. Location of HKIA and neighbouring meteorological facilities.

Under ambient easterly flows, aircraft land and depart using the 07L and 07R arrival and departure corridors (i.e. heading towards east-northeast).

anemometers for each runway. Other meteorological elements including air temperature, dew point temperature, atmospheric pressure and rainfall are measured near the middle of the airfield. Weather observations are also made by human observers at the airport.

At HKIA, surface winds are measured by three sets of

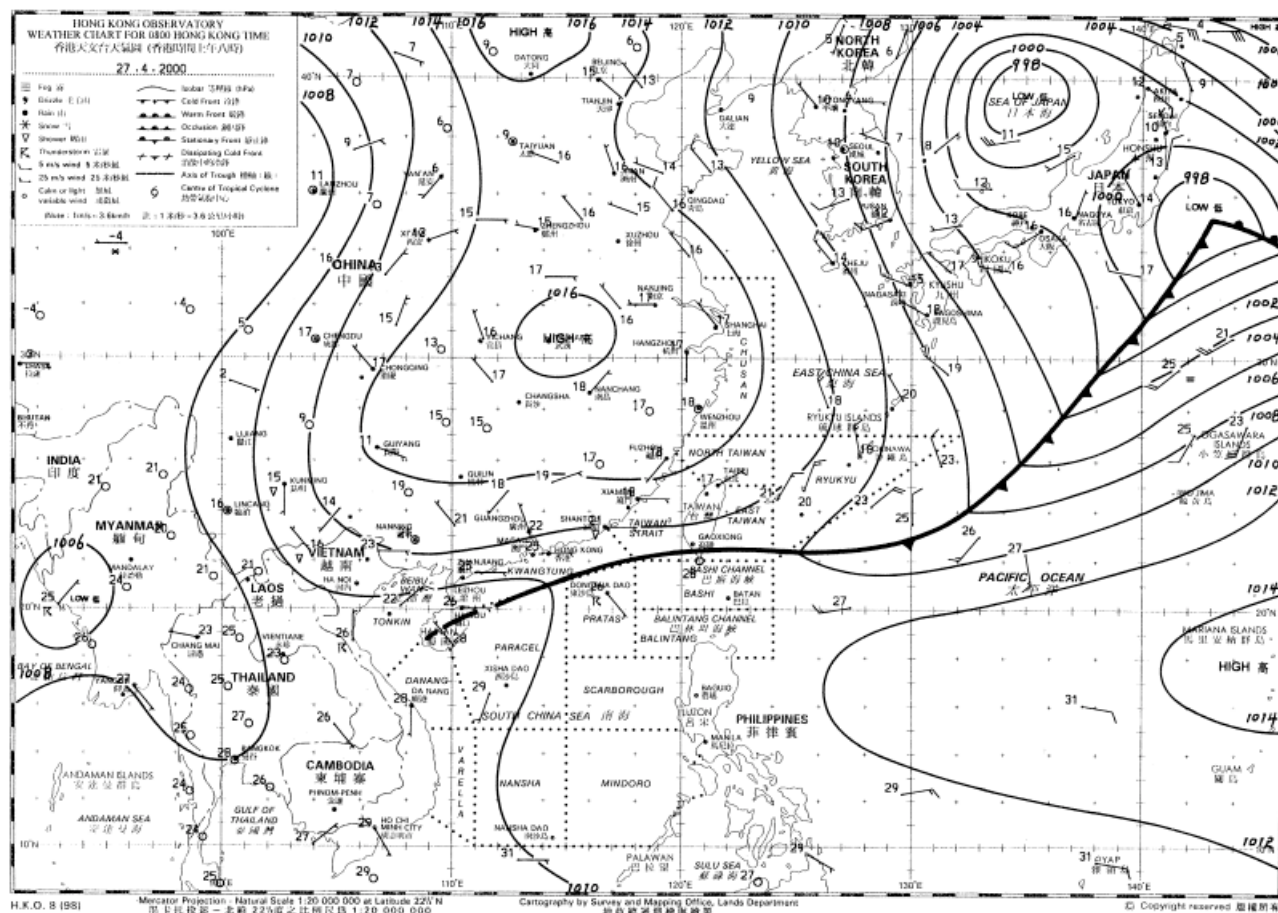


Figure 2. Daily weather map issued by the Hong Kong Observatory valid at 08 H on 27 April 2000.

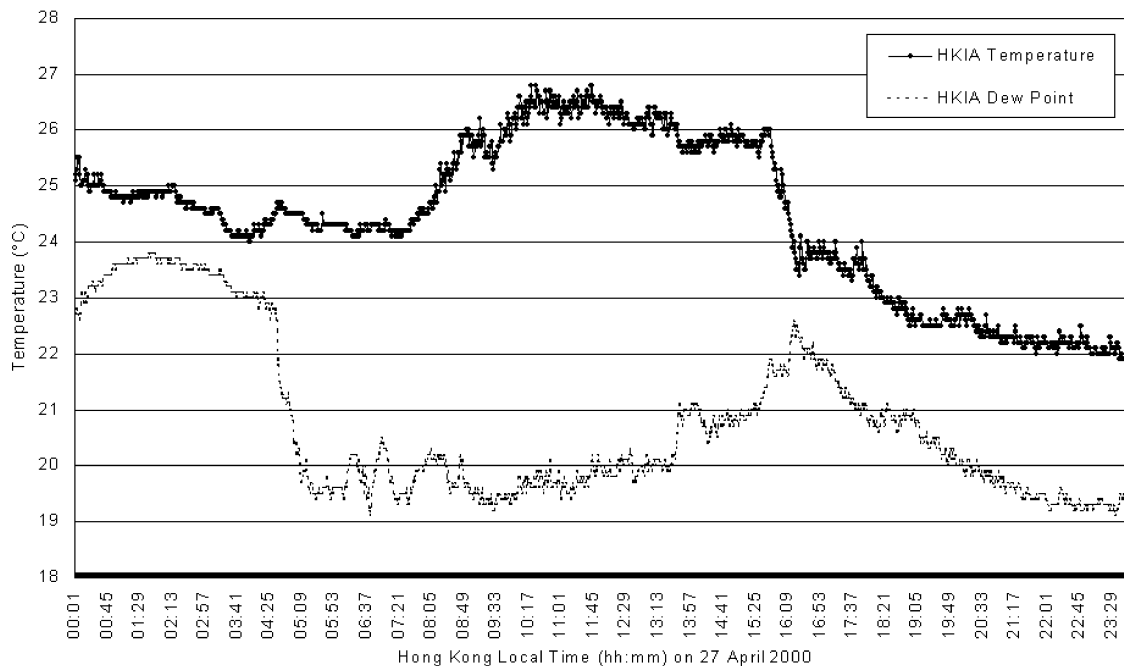


Figure 3. Time series of one-minute mean temperature and dew point at HKIA on 27 April 2000.

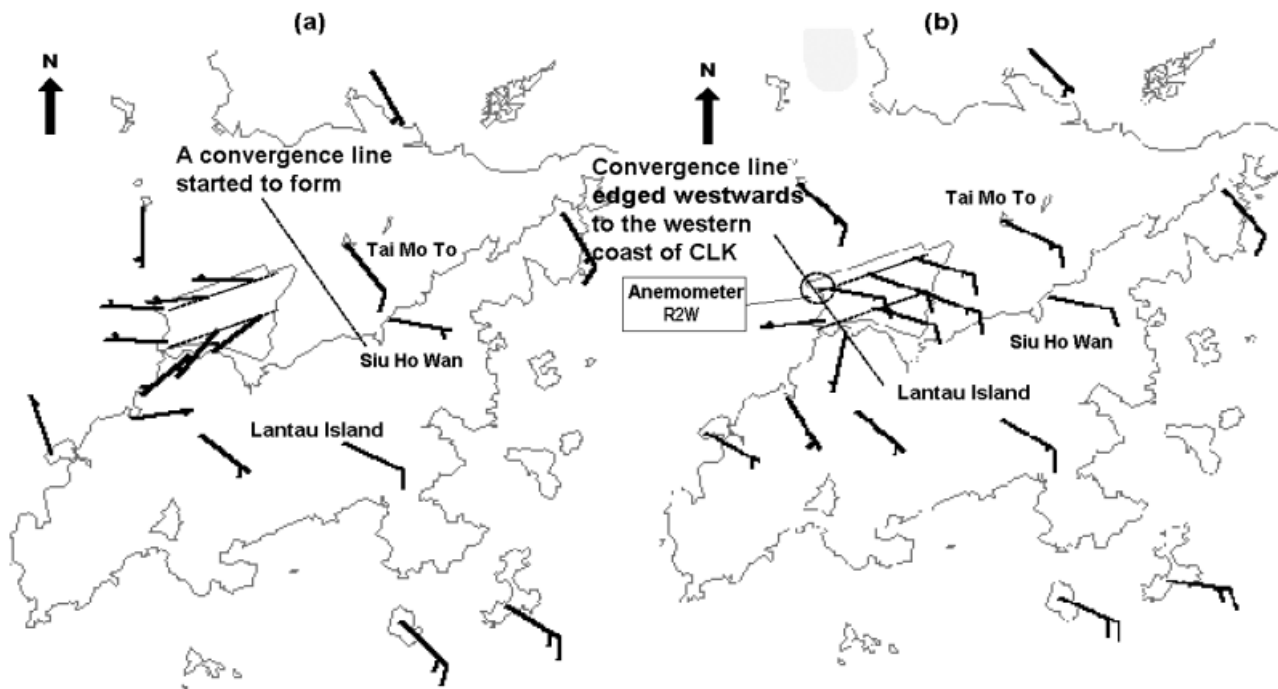


Figure 4. One-minute mean surface wind distribution at (a) 1500H; and (b) 1604H on 27 April 2000.

## 2. Sea breezes at CLK

Since CLK is an island, the sea breeze is a typical local weather system that affects the airport when there is significant temperature difference between the land and sea. A previous study (Cheng 1999) reveals that light winds or moderate east to northeasterly winds are favourable for the development of a sea breeze at the airport. Under ambient easterly flow, which is also the prevailing wind flow in Hong Kong, the sea breeze usually develops to the west of the airport, bringing a westerly flow to form a convergence zone with the opposing easterlies. The sea breeze westerlies can sometimes penetrate to the east of the airport. Towards evening, as the effects of solar heating gradually diminish, the ambient easterly flow is re-established over the airport, replacing the sea breeze westerlies.

## 3. The sea breeze on 27 April 2000

### 3.1. General weather condition

A trough of low pressure crossed the coast of southern China on 26 April 2000, leaving Hong Kong under generally cloudy conditions on 27 April. Figure 2 shows the weather chart valid at 08 H local time on that day. Showers started to affect Hong Kong in the afternoon, and in some places lasted well into the evening. Surface prevailing winds were generally from the east. Winds were light in the morning but gradually strengthened from the east in the afternoon.

### 3.2. The sea breeze front at the surface

In the morning of 27 April 2000, the weather at HKIA was fine with only 1–4 oktas of low cloud. The air temperature rose from a minimum of 24 °C to above 26 °C after 10 H local time (Figure 3), more than 3 °C above the sea surface temperature.

As the air temperature rose, sea breezes gradually set in at HKIA between 9 H and 10 H with light northwesterlies penetrating from the west (see Figure 5). Nevertheless, the dew point temperature remained at around 20 °C and did not increase until after 13 H (Figure 3). This is in contrast to the common understanding about sharp dew point changes associated with the onset of a sea breeze (Simpson 1994). This was probably related to the arrival of a dry continental airmass earlier in the morning and time was needed for this dry continental airmass to be replaced completely by the moist maritime airmass associated with the sea breeze.

A northwest–southeast oriented surface convergence line, or sea breeze front, started to form to the east of HKIA at around 15 H. As shown by the surface winds in Figure 4a, east to southeasterly winds prevailed at Siu Ho Wan and Tai Mo To, while winds over the airport remained westerlies. During the following hour, winds at Siu Ho Wan and Tai Mo To gradually strengthened from the east. With this strengthening of the easterlies the sea breeze front receded westwards across the airport. By 1604 H, the sea breeze front was already at the western edge of the airport (Figure 4b). At about the same time, an aircraft reported wind shear of 10 to 15 kt airspeed gain at a height of 30 m (100 feet) when landing on the Northern Runway from the west. While no wind shear warning was effective at the time of the report, in

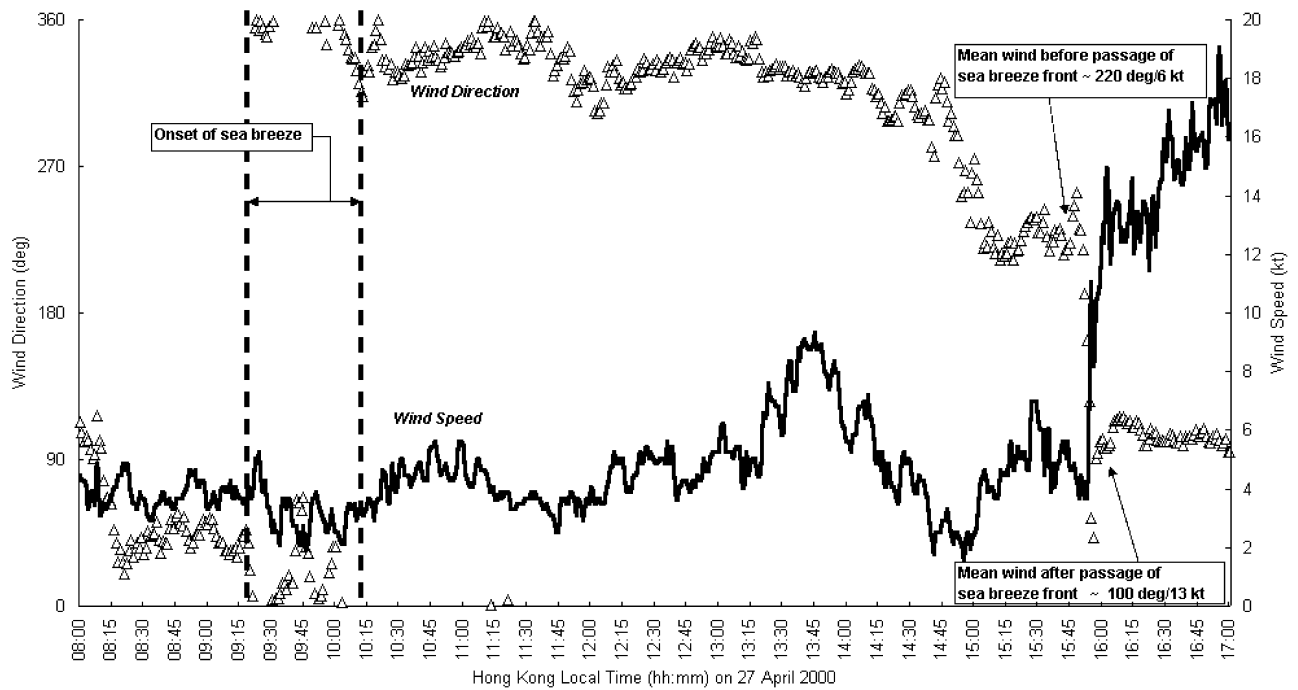


Figure 5. Time series of wind direction and speed recorded by anemometer R2W during sea breeze front onset and retreat.

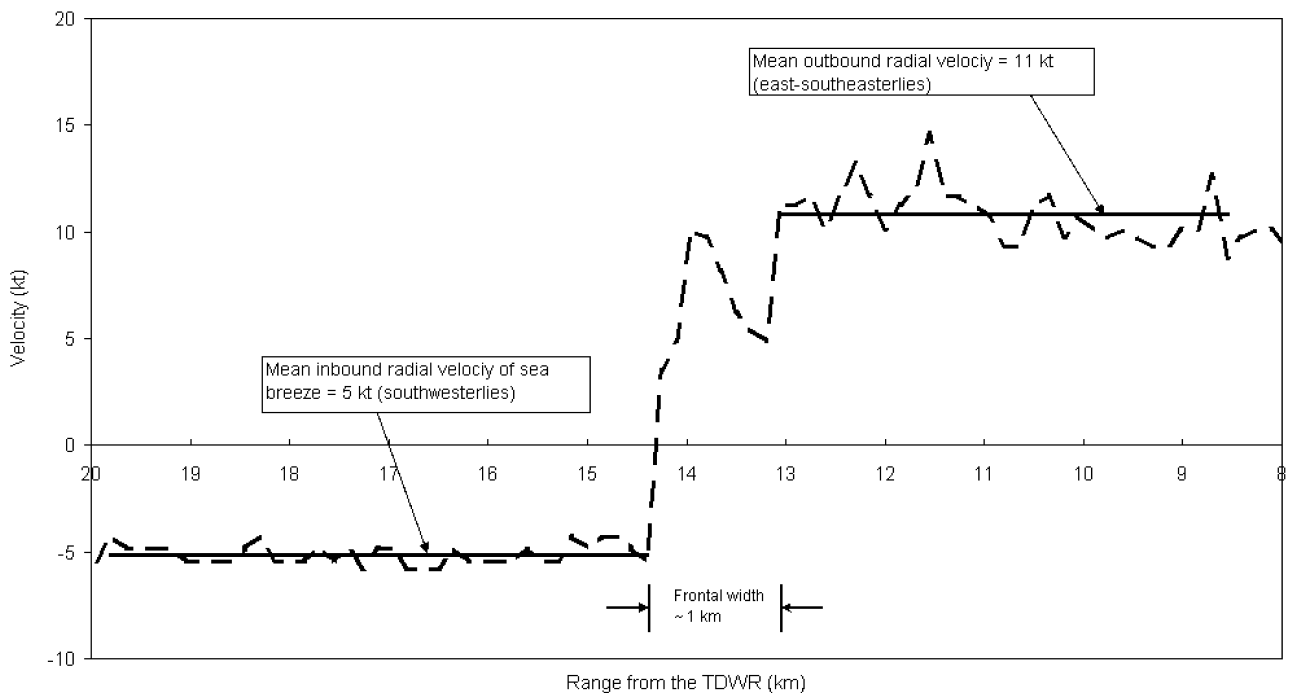


Figure 7. TDWR Doppler radial velocity against radar range at 0.6 degree elevation at beam azimuth of 244 degrees at 1604H on 27 April 2000.

view of the proximity of the sea breeze front to the aircraft touchdown location, it is likely that the reported wind shear was caused by the convergence between the strengthening easterlies and the sea breeze westerlies.

To assess the wind change across the sea breeze front, the time series of one-minute mean wind recorded by the anemometer at the aircraft touchdown location (labelled as ‘Anemometer R2W’ in Figure 4b) was examined (Figure 5). A significant change of winds associated with the retreat of the sea breeze front can be seen

from 1548 H to 1600 H, shortly before the wind shear reporting time of 1604 H. The anemometer winds resolved along the runway direction (positive sign representing head wind for the aircraft landing towards 070 degrees, negative sign representing tail wind) immediately before and after the passage of the sea breeze front are estimated from the data in Figure 5 to be about  $-5$  kt and  $+11$  kt respectively. The head wind change across the sea breeze front is therefore estimated to be about  $+11 - (-5)$  kt =  $+16$  kt which agrees well with the reported wind shear of 10 kt to 15 kt airspeed gain.

Figure 6(a)

Figure 6(b)

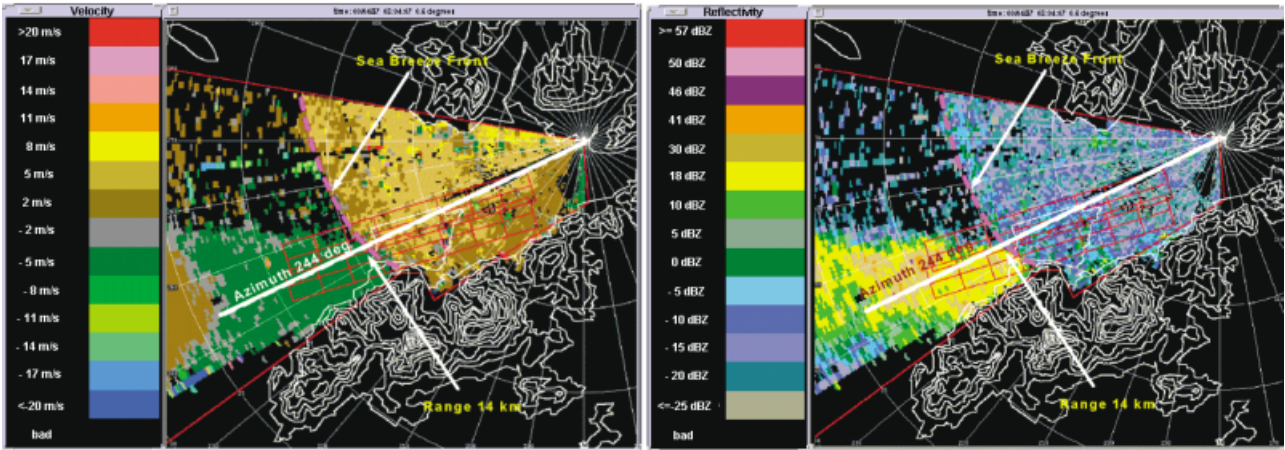


Figure 6. (a) Doppler radial velocity; and (b) reflectivity at 0.6 degree elevation at 1604 H on 27 April 2000. Colour Plate I.

Figure 8(a)

Figure 8(b)

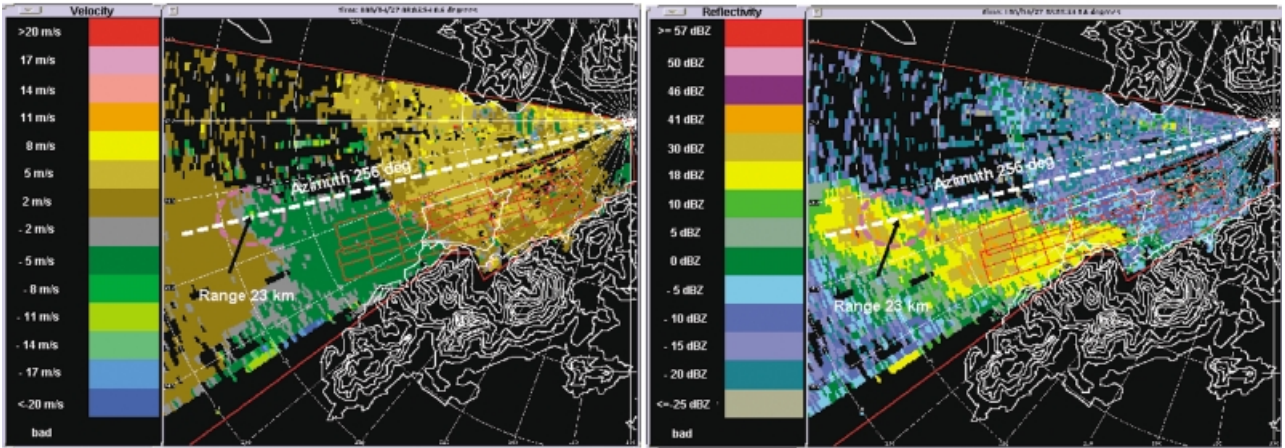


Figure 8. (a) Doppler radial velocity; and (b) reflectivity at 0.6 degree elevation at 1606 H on 27 April 2000. Colour Plate I.

The aligned 'green' region with lower reflectivity around 10 dBZ compared to showers generally above 30 dBZ is caused by the clutter filter which notches signals that have Doppler shift between  $-2 \text{ m/s}$  and  $+2 \text{ m/s}$ .

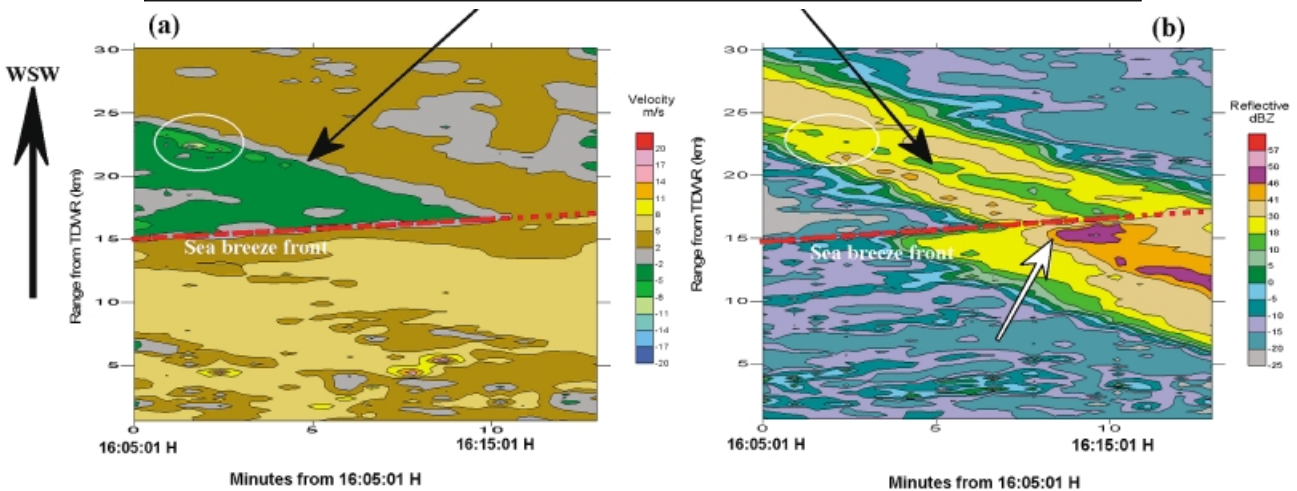


Figure 9. Hovmuller diagrams of: (a) Doppler radial velocity; and (b) reflectivity at 0.6 degree elevation and 256 degrees azimuth from 1605 to 1618 H on 27 April 2000. Colour Plate I.

Figure 5 also reveals a significant increase in strength of the easterlies compared with the southwesterlies, suggesting that the westward movement of the sea breeze front was the result of the strengthening easterlies rather than a normal diurnal retreat of the sea breeze. It is also interesting to note that while the air temperature dropped by more than 2 °C during the passage of the sea breeze front at around 16 H, the dew point temperature peaked shortly after 16 H before dropping to pre-sea breeze values (Figure 3), indicating moisture convergence near the sea breeze front.

### 3.3. The sea breeze front as observed by the TDWR

The passage of the sea breeze front around the time of the reported wind shear event was also clearly observed by the TDWR. The TDWR is a Doppler weather radar developed by the US Federal Aviation Administration (FAA) in the 1980s for automatic detection and warning of microburst and wind shear associated with convective storms (Turnbull et al. 1989). Forty-five TDWR systems have been deployed at US airports. The TDWR in Hong Kong is the first such system installed outside America (Shun & Johnson 1995; Johnson et al. 1997). The TDWR is located at about 12 kilometres northeast of HKIA (Figure 1). Operating in the C band, the TDWR has a narrow 3 dB beamwidth of 0.55 degrees. It utilises a highly stable klystron-based amplifier and sophisticated algorithms for effective filtering of stationary and moving clutters. Although the TDWR was designed to detect microburst and wind shear in rainy conditions, it is highly sensitive and is sometimes able to provide high-resolution data in clear air conditions, such as those on days with sea breezes.

Figure 6 (in Colour Plate I) shows the TDWR Doppler radial velocity and reflectivity at 0.6 degree elevation at 1604 H, the time of the reported wind shear event. From the Doppler velocity data (Figure 6a), a north-west–southeast oriented convergence line can be clearly identified (highlighted as a magenta dashed line), with outbound velocities to the east of the front and inbound velocities to the west of the convergence line. From the reflectivity data (Figure 6b), a ‘thin line’ of elevated clear air reflectivity (in the region of –5 dBZ) is also discernible from the background reflectivity (as low as –20 dBZ) just to the east of the convergence line. The area of higher reflectivity (up to around 30 dBZ) to the southwest of the convergence line is associated with approaching convection, which will be discussed in section 4 below. Note that the Doppler velocity pattern associated with the convergence line was not altered by the approach of the convection as can be seen by comparing Figures 6a and 8a in Colour Plate I.

The magnitude of convergence at the sea breeze front can be estimated by considering the Doppler radial

velocity of a single radar beam traversing the front. Figure 7 is a graph of the Doppler radial velocity against radar range at 0.6 degree elevation at beam azimuth of 244 degrees at 1604H on 27 April 2000 (marked as a white line in Figure 6). This beam was chosen by virtue of its proximity to the reported wind shear location and good radar data availability. From Figure 7, the outbound (positive) Doppler velocity associated with the ambient easterlies (at radar ranges less than 13 km from the TDWR) was estimated to be about 11 kt (6 m/s). At longer ranges (more than 15 km from the TDWR), the inbound Doppler radial velocity associated with the southwesterly sea breeze was generally about 5 kt (3 m/s). This gives a wind change of about 16 kt (8 m/s) across the sea breeze front. With an estimated frontal width of about 1 km, the convergence at the sea breeze front may be estimated to be about 8 m/s/km or  $8 \times 10^{-3}$  /s. Since the radar beam more or less aligns with the orientation of the runways (244 degrees versus 250 degrees), it can be concluded that the radar-derived wind change agrees well with that estimated from the anemometer data (also 16 kt) and the reported wind shear of 10 to 15 kt experienced by the aircraft. The agreement suggests that the convergence of the sea breeze front was rather uniform in the lowest 200 m, as the height of the radar beam at 0.6 degree elevation over anemometer R2W is about 210 m above mean sea level and the height of the aircraft-reported wind shear was about 30 m (100 ft).

## 4. Interaction between sea breeze and convection

An area of showers developed near the coast of southern China in the vicinity of the trough of low pressure (see Figure 2) and moved in from the southwest. The showers interacted with the sea breeze front after 16 H. From the TDWR Doppler velocity data at 0.6 degree elevation at 1606 H (Figure 8a in Colour Plate I), a small area of significant radial divergence (highlighted by a magenta ellipse in Figure 8a) can be identified within the area of showers with over 30 dBZ reflectivity (Figure 8b in Colour Plate I). The radial divergence was apparently a result of outbound velocity of about 2 m/s at longer radar range (> 25 km) and inbound velocity in excess of 8 m/s at shorter radar range (at about 23 km), giving a velocity difference of about 10 m/s over a distance of just a couple of kilometres. Aircraft flying across this divergence would experience significant low-level wind shear with airspeed loss.

The temporal evolution of the interaction between the convection and sea breeze front can be illustrated by Hovmuller diagrams of Doppler radial velocity and reflectivity for an intersecting radar beam at 0.6 degree elevation. A Hovmuller diagram is a two-dimensional plot of a parameter against space and time. In this case a Hovmuller diagram of the Doppler radial velocity or reflectivity for a single radar beam shows the variation

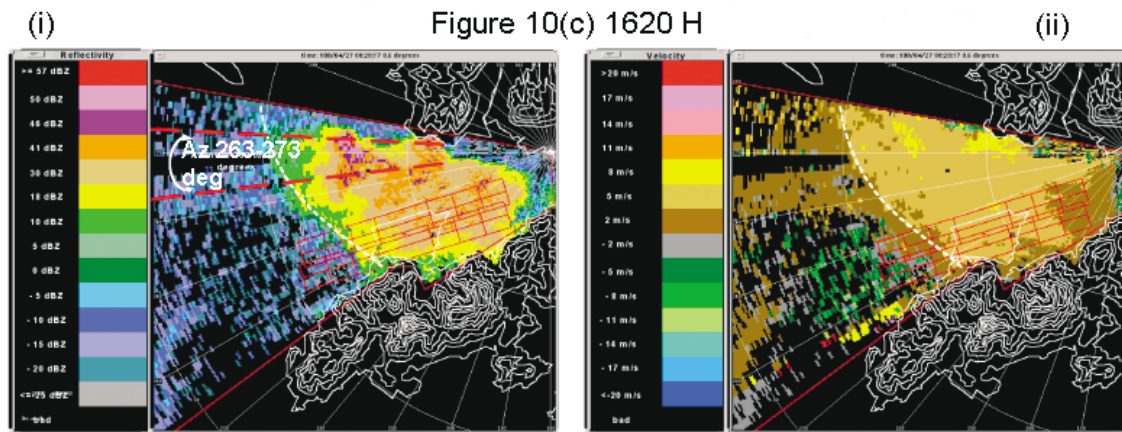
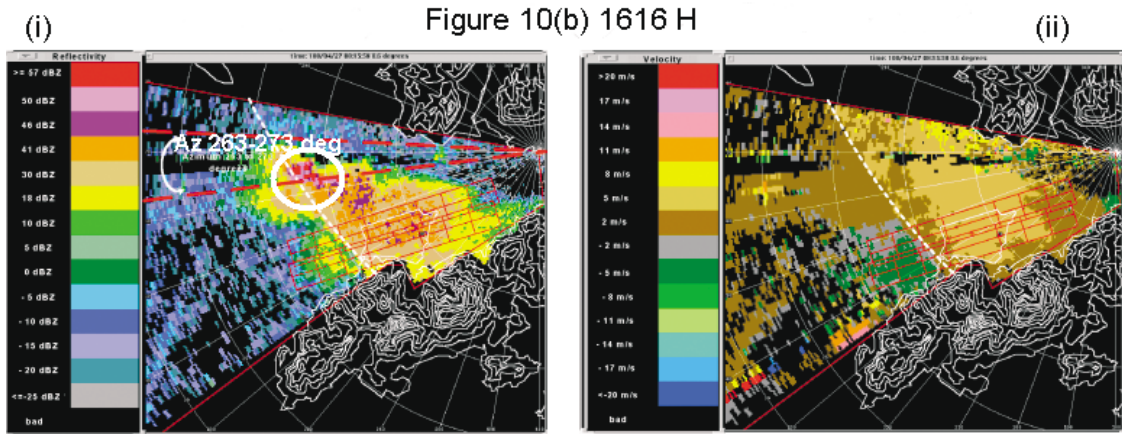
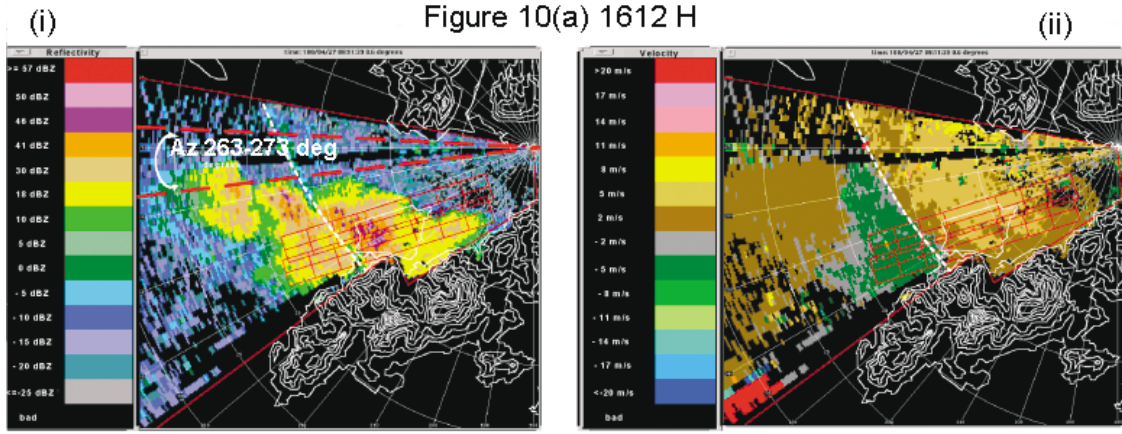


Figure 10. (i) Reflectivity; and (ii) Doppler radial velocity at 0.6 degree elevation at: (a) 1612 H; (b) 1616 H; and (c) 1620 H on 27 April 2000. Note the apparent intensification of reflectivity (highlighted by the white circle in Figure 10b(i)) when showers crossed the sea breeze front (denoted by white dotted line) Colour Plate II.

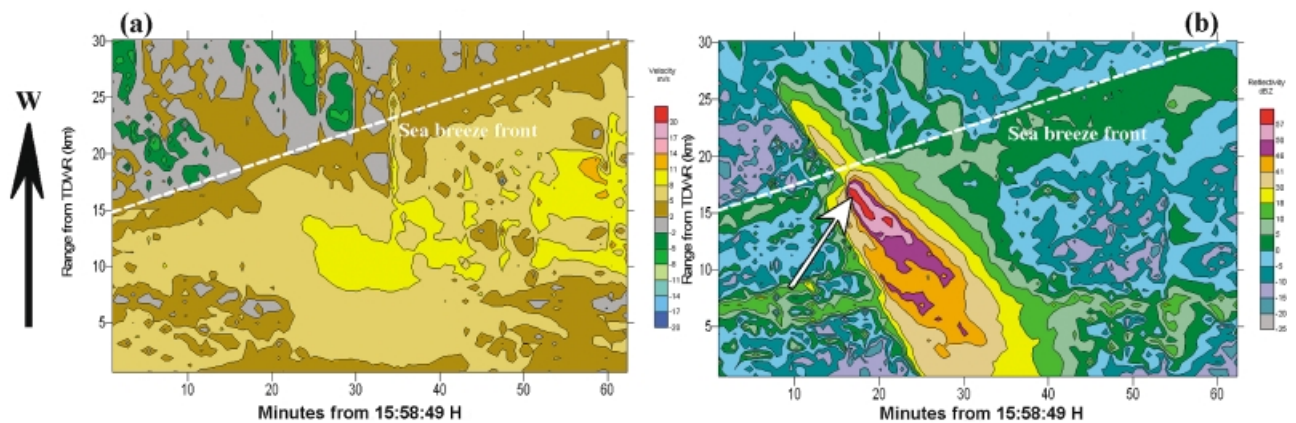


Figure 11. Hovmuller diagrams of: (a) mean Doppler velocity; and (b) maximum reflectivity within the azimuth 263 to 273 degrees for the period from 1558 to 1701 H on 27 April 2000. Colour Plate II.

of Doppler radial velocity or reflectivity in radar range and time. The radar beam azimuth of 256 degrees (marked as a white dashed line in Figure 8) is chosen for the Hovmuller diagrams in Figure 9 (see Colour Plate I), with the horizontal axis representing increasing time and the vertical axis representing increasing range from the TDWR.

The Hovmuller diagrams reveal a number of interesting features:

- (a) The significant radial divergence (highlighted by the white ellipse in Figure 9a) was apparently associated with a convective cell to its immediate west, i.e. at a slightly longer range (between 25 and 28 km at 1605 H), as both features moved at an average speed of about 13 m/s towards the radar. However, the radial divergence only lasted several minutes and quickly diminished as this convective cell weakened. Another convective cell started to develop to its immediate east, i.e. at a slightly shorter range (at around 21 km at 1607 H) when the radial divergence was at its maximum.
- (b) The sea breeze front, marked by the radial convergence between inbound and outbound Doppler radial velocities (highlighted by the red dotted line in Figure 9a), was moving at an average speed of about 2 m/s away from the radar. The sea breeze front also appears as a line of discontinuity in the reflectivity field in Figure 9b. In particular, a marked increase in reflectivity (from around 30 dBZ to over 46 dBZ) can be seen around 1614 H (highlighted by a white arrow in Figure 9b). This enhancement of reflectivity will be discussed in more detail below.
- (c) The radial coverage of the inbound radial velocity shrank in size as the convection approached the sea breeze front. The inbound radial velocity associated with the sea breeze westerlies was apparently eroded by the outbound radial velocity brought by the convection.

One point to note when interpreting the reflectivity data in Figure 9b is that due to clutter filtering of stationary scatterers, reflectivity return will appear low whenever the corresponding Doppler radial velocity falls within  $\pm 2$  m/s. The aligned 'green' region marked in Figure 9b and, to a certain extent, the reflectivity discontinuity at the sea breeze front are results of the clutter filtering.

The enhancement of reflectivity described in point (b) above can be better visualised in Figure 10 (in Colour Plate II). Note in particular the marked intensification at and after 1616 H (Figures 10b(i) and 10c(i)). The enhancement is believed to be due to the low-level wind and moisture convergence associated with the sea breeze front, which is identified in Figures 10a–10c as a boundary with significant change of Doppler radial velocity and clear-air reflectivity across it.

The enhancement of reflectivity could be elicited by Hovmuller diagrams of reflectivity and Doppler radial velocity (Figure 11 in Colour Plate II). In Figures 11a and 11b, the horizontal axis represents increasing time and the vertical axis represents increasing range from the TDWR. Figure 11b is the Hovmuller diagram of maximum reflectivity over radials between azimuth angles of 263 to 273 degrees (inclusive) at a given range. The location of this 10-degree sector is shown in Figure 10. This sector is chosen to illustrate the enhancement of reflectivity in view of the better reflectivity return within this sector. Figure 11a is the Hovmuller diagram of mean Doppler radial velocity over radials between azimuth angles of 263 to 273 degrees (inclusive) at a given range. Figure 11b reveals that the convection with reflectivity initially around 30 dBZ intensified to over 50 dBZ after crossing the sea breeze front (see intensification zone highlighted by a white arrow). The sea breeze front shows up as a boundary with significant change in clear-air reflectivity and radial velocity across it. In particular, slightly higher level of clear-air reflectivity up to about 10 dBZ (compared with the lower background of below 0 dBZ) can clearly be seen just on the radar side of the sea breeze front. Convergence of Doppler radial velocities at the sea breeze front is also evident, especially during the first 30 minutes or so, i.e. between 1558 H and 1628 H. While the convection moved at an average radial speed of about 13–16 m/s towards the radar, the sea breeze front was retreating away from the radar at an average radial speed of about 3–4 m/s. These values are consistent with those noted in the discussions pertaining to Figure 9 above.

## 5. Conclusion and remarks

The present analysis shows how a sea breeze, when interacting with other weather phenomena such as strengthening background winds and approaching convection, can trigger other interesting weather events including low-level wind shear to aircraft and enhanced convective development. Detailed analysis of these phenomena is not possible with conventional meteorological data. The implementation of the TDWR has made available high-resolution observational data of reflectivity and Doppler radial velocity. The present study has demonstrated that the TDWR, apart from detecting and warning of low-level wind shear and microburst in rainy conditions, is capable of providing better understanding of such mesoscale systems as sea breeze circulations and their interactions with other systems, thus improving mesoscale weather nowcasting. With experience gained from this study, weather forecasters now make routine use of the TDWR data in clear air conditions, when available, to issue wind shear alerts to aircraft landing at or taking off from HKIA, supplementing those generated by automatic systems.

## References

- Cheng, C. M. (1999) Characteristics of Sea Breezes at Chek Lap Kok, *Hong Kong Observatory Technical Note No. 96*. Hong Kong Observatory, 23 pp.
- Johnson, D. B., Keeler, R.J., Kessinger, C., Shun, C. M., Wilson, P. & Wieler, J. G. (1997) Optimization and testing of a Terminal Doppler Weather Radar for the new Hong Kong International Airport at Chek Lap Kok. *Preprints, 28<sup>th</sup> Conf. on Radar Meteorology (Austin, Texas)*, American Meteorological Society, Boston, 174–175.
- Shun, C. M. & Johnson, D. B. (1995) Implementation of a Terminal Doppler Weather Radar for the new Hong Kong International Airport at Chek Lap Kok. *Preprints, Sixth Conf. on Aviation Weather Systems (Dallas, Texas)*, American Meteorological Society, Boston, 530–534.
- Simpson, J. E. (1994) *Sea Breeze and Local Wind*. Cambridge University Press, 234 pp.
- Turnbull, D., McCarthy, J., Evans, J. & Zrnic, D. (1989). The FAA Terminal Doppler Weather Radar (TDWR) program. *Preprints, Third Int. Conf. on Aviation Weather Systems (Anaheim, California)*, American Meteorological Society, Boston, 414–418.